Computationally efficient method for determining the most important electrical parameters of axial field permanent magnet machine

A. SMOLEŃ and M. GOŁĘBIOWSKI*

Warsaw University of Technology, ul. Koszykowa 75, 00-662 Warsaw, Poland

Abstract. This paper describes a numerically efficient method for determining the electrical parameters of axial field permanent magnet machine (AFPM). The presented method aims to accurately determine the back EMF waveform and self-inductance coefficients, while maintaining possibly low computational complexity, which is crucial in case of incorporation of the method in numerical optimization procedure of AFPM construction. The described algorithm is based on 2D FEM with several simplifications. The obtained results have been compared with full 3D FEA conducted with Ansys/Maxwell software, and confirmed by measurements. The result shows that presented method ensures satisfactory accuracy as well as computational time performance.

Key words: axial flux permanent magnet, 2D FEA, numerical optimization.

1. Introduction

The coreless axial flux permanent magnet machines, are becoming more and more popular in many industrial applications. The construction, characterized by huge ratio of machine diameter to its axial length, makes it particularly suitable to mechanical integration with vertical axis wind turbines or internal combustion engines. Because of the absence of core losses, such types of machines can potentially achieve higher efficiency. A wide range of possible applications causes various demands when it comes to design process, especially if the goal is to obtain the constructions dedicated for a particular application. In purpose of design the machine which reveals desired dynamic properties, it is necessary to determine geometry of the machine, which provides proper values of its electrical parameters. In dynamic properties, point of view the most important electrical parameters are back EMF waveform and self inductance coefficients. To determine these values for given geometry of the machine, the magnetic field distribution inside of AFPM machine needs to be calculated. So far, most of published works proposed an approach that uses analytical methods to calculate this distribution for a simplified 1D model [1–3]. Based on these results, the optimization criteria (usually a single variable objective function) have also been minimized by using analytical methods [4]. The limitations of such approach are mostly related to the number of optimization variables, which in some cases, needs to be greater than one, as well as to the accuracy of 1D simplified model of magnetic field distribution [5]. On the other hand, there is a possibility to conduct very accurate optimization calculations based on 3D FEA of magnetic field distribution inside AFPM machine. The main drawback of this

approach is high computational complexity, which makes the process extremely time/computational power consuming. It was pointed out in the literature [6, 7] that 2D FE models also give a very accurate representation of magnetic field distribution in AFPM machine. There are some works published, which discuss the concept of incorporating 2D FE calculations in the numerical optimization procedure applied to design process of AFPM machine [8], however, there are no published works which aim to assess the accuracy of these methods in case of determining particular electrical parameter of AFPM machine. The assessment aims to determine the scope of applicability of 2D approach when it comes to numerical optimisation of AFPM construction. The computational efficiency of evaluation of the value of objective function has a great importance especially if some modern optimisation algorithms, such as PSO or ABC, are going to be used. When it comes to accuracy versus time consumption,the simulation and experimental tests have been performed to find the most suiTable algorithm of determining the most important electrical parameters of AFPM machine. The analytical approach was also considered, but simulation tests showed that time performance is worse than in case of numerical computations.

In this paper the chosen method, based on simplified 2D FE algorithm, is presented and compared with results of full 3D FEA conducted by using Ansys/Maxwell software as well as the results of experimental tests conducted on a machine prototype. The assessment of accuracy and computational time of presented simplified algorithm has been provided.

2. Statement of computational problem and model description

2.1. AFPM machine model. The coreless AFPM machine consists of a single stator disc fixed in the middle and two outer rotor discs with surface mounted permanent magnets. The stator

coils are radially placed and the magnetic field is in axial direction. The machine available for experimental tests has a 2.8 kW rated power and 32 uniformly distributed, rectangularly shaped permanent magnets, mounted on each of the rotor discs. The positioning of the magnets is alternating, which gives 16 pole pairs. A schematic drawing of machine construction is presented in Fig. 1.
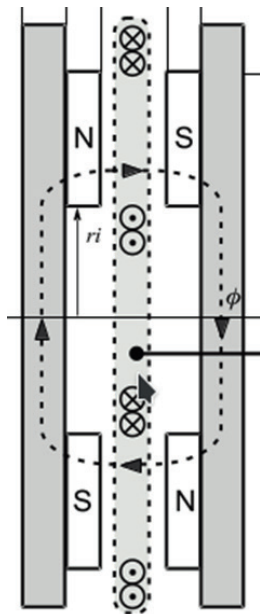

Fig. 1. The schematic cross section representing a single pole pitch of the core less AFPM machine

The stator winding is a three phase overlapping type and it consists of 16 uniformly distributed, series connected, rectangularly shaped coils per phase. Subjected construction is a coreless type, which means that there is no iron in a stator disc and the winding is kept in place by encapsulation in epoxy resin. The influence of magnetic permeability of such material can be neglected, which lets us omit this domain in FE model and effectively reduce a total number of nodes. Moreover, due to relatively huge air gap, there is no magnetic saturation phenomenon which allows us to apply further simplifications to 2D FE procedure. The 2D FE model of the machine is a flat layout of cylindrical cutting surface placed in the middle of stator coil active part, which is presented in Fig. 2. The geometrical dimensions of cutting plane in meters are labelled on graph axis. The 2D FEA is inherently unable to fully handle a magnetic field distribution in the overlapping end connection region of stator winding. Only a single pole pitch section has been chosen to 2D calculations. However, in case of 3D calculations, two pole pitches have been analysed to handle all properties of magnetic field distribution [9].

In FEM, the whole domain is divided in a sub domains with a specific physical properties and loads assigned to them. In a presented model, the domains number 2 and 5 are solid steel rotor yoke planes. Sub areas number 3, 4, 6, 7 are the
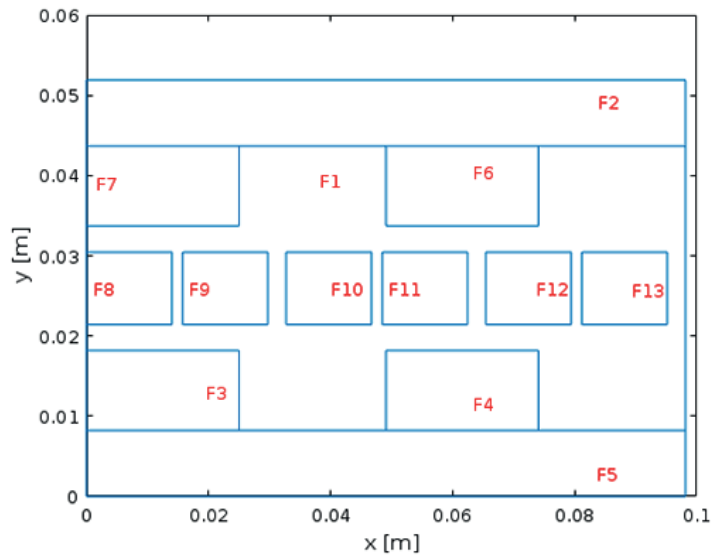

Fig. 2. A flat layout of machine cross section on a single pole pitch – the model for a 2D FEA

neodymium magnets, and sub areas from 8 to 13 are the coils cross sections arranged with a following order: A^-, C^+, B^-, A^+, C^-, B^+ where each letter denotes the phase and each sign denotes a direction of current flow. Construction parameters of considered AFPM machine relevant for 2D field calculations have been presented in Table 1 The machine model can be set in cartesian coordinates, because the radius of the machine is huge in comparison to the width of the air gap [10].

Table 1
Machine model parameters

parameter	value	unit
rotor yoke plane		
rotor yoke thickness	8	mm
axial distance between yokes	35	mm
material	steel s235	[–]
permanent magnets		
width	25	mm
high	10	mm
averaged induction remanence B_r	1.19	T
relative magnetic permeability μ_r	1.0922	[–]
stator coils		
radial length	85	mm
angular width	240	elec. deg
cross section width	14	mm
cross section high	9	mm
number of wires	64	[–]
coil active length	0.0502	m

www.czasopisma.pan.pl   PAN   www.journals.pan.pl

Computationally efficient method for determining the most important electrical parameters of Axial Field Permanent Magnet machine

2.2. Computational problem. To determine the values of machine inductance coefficients, the distribution of magnetic field, generated by each phase current individually, needs to be calculated. While conducting these calculations, the influence of permanent magnets isn't considered. In order to apply a 2D analysis to a presented problem, the symmetry along z axis is assumed. Because of its source-less nature the magnetic induction field $\vec{B}$ can be represented as a rotation of vector potential $\vec{A}$

$$div\vec{B} = 0 \Rightarrow div(rot\vec{A}) = 0 \Rightarrow \vec{B} = rot(\vec{A}). \quad (1)$$

The mentioned symmetry assumption causes that the vector of current density $\vec{J}$ has only a z component. Applying Maxwell first equation:

$$rot\vec{H} = \left(\frac{1}{\mu}rot\vec{A}\right) = \vec{J} = (\overrightarrow{0,0,j_z}). \quad (2)$$

Hence the vector potential $\vec{A}$ also has only that component

$$\vec{B} = rot(\vec{A}) = \begin{bmatrix} \vec{i}, & \vec{j}, & \vec{k} \\ \frac{\partial}{\partial x} & \frac{\partial}{\partial y} & \frac{\partial}{\partial z} \\ 0, & 0, & A_z(x,y) \end{bmatrix}. \quad (3)$$

The components of magnetic induction field $\vec{B}$ on a considered $x - y$ plane are given by:

$$B_x = \frac{\partial}{\partial y}A_z(x,y); \;\; B_y = -\frac{\partial}{\partial x}A_z(x,y). \quad (4)$$

Substituting the component mentioned above to the equation 2 and writing all in the open form

$$\begin{bmatrix} \vec{i}, & \vec{j}, & \vec{k} \\ \frac{\partial}{\partial x} & \frac{\partial}{\partial y} & \frac{\partial}{\partial z} \\ \frac{1}{\mu}\frac{\partial}{\partial y}A_z(x,y), & -\frac{1}{\mu}\frac{\partial}{\partial x}A_z(x,y), & 0 \end{bmatrix} = \vec{k}\cdot J_z. \quad (5)$$

The equation which needs to be solved using FEM is then given by z $(\vec{k})$ component.

$$\frac{\partial}{\partial x}\left(\frac{1}{\mu}\frac{\partial}{\partial x}A_z\right) + \frac{\partial}{\partial y}\left(\frac{1}{\mu}\frac{\partial}{\partial y}A_z\right) = -J_z \quad (6)$$

In order to calculate the magnetic flux coupled with a stator winding, the distribution of magnetic field generated by permanent magnets under no current conditions needs to be computed. The purpose of the efforts was to develop, test and validate the code which can be later incorporated in a numerical optimization procedure, and used without any sophisticated software tools. For this reason, the 2D FEM code for solving presented problem has been implemented in Matlab from scratch. The geometry model has been prepared as a *.dxf* file using AutoCad software, and imported to Matlab. For mesh generation, the

open sources package provided in [11] was used. To achieve the lowest possible computational complexity the linear basis functions have been chosen. The overall computational methodology has been presented in great details in [12–15].

2.3. Applying boundary conditions. Since the rotor yokes are made of solid iron, which has a magnetic permeability about 4000 times higher than the air, it can be expected that there is no magnetic field flow outside the yoke plate to the air. For this reason, the zero value of Dirichlet boundary condition needs to be applied on the outside edges of yoke sub domains. It can be easily achieved by applying zero value for all elements in rows of the main matrix, corresponding to the nodes laying on those edges, applying value 1 to its diagonal elements and the value 0 to a corresponding element of the load vector. Due to symmetry, for reducing the computational complexity only the part of machine cross section is analysed. For this reason, the special matching boundary condition needs to be applied on the vertical boundaries of the considered domain presented in Fig. 2. In order to respect the symmetry of the machine, it needs to be forced that the values of vector potential obtained for the left edge of the domain are equal to these obtained for its right edge. In a discussed procedure, the unstructured triangular mesh is used, which leads to disproportionate numbers of nodes laying on left and right edges. For this reason, the edge containing greater number of nodes, needs to be chosen as a dominating one and the matrix of weight coefficients needs to be determined to achieve equal values obtained for nodes laying on subordinate edge to a weighted average of values obtained for the two nearest nods to them in vertical direction but lying on dominating edge. The weight coefficients are determined based on distance between dominating nodes and a subordinate one, as follows:

$$W_1 = \frac{|y_{d1} - y_s|}{|y_{d1} - y_s| + |y_{d2} - y_s|} \quad (7)$$

$$W_2 = \frac{|y_{d2} - y_s|}{|y_{d1} - y_s| + |y_{d2} - y_s|} \quad (8)$$

where: y_{d1} and y_{d2} are the y coordinates of the nodes lying on dominate edge. y_s is the y coordinate of the node lying between y_{d1} and y_{d2}, but on a subordinate edge.

To efficiently apply this boundary condition, it is convenient to create a matrix multiplier, which consists of unity part to preserve the structure of the main matrix and the set of rows corresponding to subordinate nodes with the weight coefficients located in columns corresponding to the location of dominating nodes.

$$\mathbf{Z} = \begin{bmatrix} 1 & 0 & 0 & 0 & 0 & \cdots & 0 \\ 0 & 1 & 0 & 0 & 0 & \cdots & 0 \\ \vdots & & \ddots & & & & \\ W_1 & 0 & \cdots & W_2 & & \cdots & 0 \\ \vdots & & & & & & \end{bmatrix} \quad (9)$$

It needs to be pointed out that before using matrix multiplier in a presented form, the main matrix of the system needs to be reordered in such a way that the rows corresponding to subordinate nodes are collected at the bottom. The system of linear equations, obtained from activities described previously, has a following form:

$$\mathbf{M}\bar{u} = \bar{L}. \tag{10}$$

After applying Dirichlet boundary conditions, the following operations need to be done.

$$\mathbf{A} = \mathbf{Z^T}\{\mathbf{R^T MR}\} \tag{11}$$

where $\mathbf{R}$ is a reordering matrix, which makes the main system matrix organized in such a way that matrix multiplier Z can be used in a form presented above

$$\bar{b} = \mathbf{Z^T R^T}\bar{L} \tag{12}$$

$$\mathbf{A}\bar{u}_P = \bar{b}, \quad \bar{u}_p \neq \bar{u} \tag{13}$$

where $\bar{u}_p$ is the new, shorted and reordered vector of unknowns. It should be emphasised that, after presented manipulations were implemented, the dimension of the system of linear equations has been decreased by the number of subordinated nodes.

2.4. Solving the system of linear equations. Due to high demands on reducing computational complexity of presented algorithm, as well as the dimension of $\mathbf{A}$ matrix which can be potentially large, only the iterative methods of solving the systems of linear equations have been considered. If it comes to consumption of computational time, the matrix conditioning is crucial. The structure of obtained the sparse matrix $\mathbf{A}$ is presented in Fig. 3.
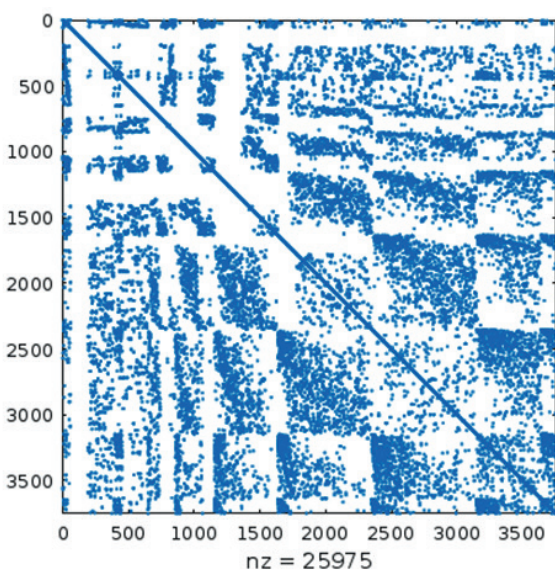

Fig. 3. The structure of linear system matrix after applying a boundary condition

The Generalized Minimum Residual Method has been chosen to use for solving the system. Regarded to the literature, it is the best suited method for the sparse nonsymmetric linear systems [16]. To assess the initial situation, a convergence test has been conducted without any preconditioning. Resulting convergence plot is presented in Fig. 4.
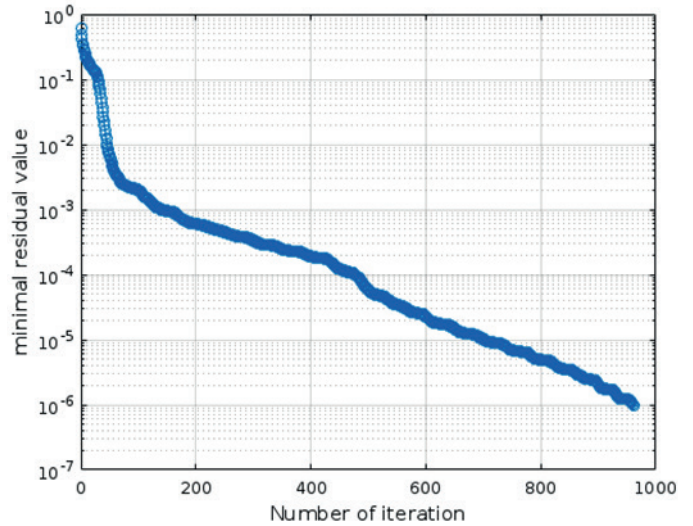

Fig. 4. Minimum residual values obtained for solving a system without preconditioning

The results showed that satisfactory value of residue is obtained after more than nine hundred iterations of GMR, which is unacceptably time-consuming. Due to the fact that after applying the Cuthill-McKee permutation, the matrix A became diagonally dominated thus the starting point for a GMR iterations has been chosen as 14

$$\hat{\bar{u}}_p = \begin{bmatrix} A_{1,1} & & \\ & \ddots & \\ & & A_{np,np} \end{bmatrix}^{-1} \cdot \begin{bmatrix} b_1 \\ \vdots \\ b_{np} \end{bmatrix}. \tag{14}$$

To further improve the convergence rate, the Incomplete LU factorization method has been applied with a tolerance parameter equal to $1 \cdot 10^{-6}$. Conducted simulation tests showed, that it gives excellent improvement in the convergence rate and effectively decreases the computational complexity of overall developed code. The plot of GMR convergence after described preconditioning process is presented in Fig. 5.

By solving the linear system, the shortened vector $\bar{u}_p$ is calculated. To determine the values of the vector potential $\vec{A}$, corresponding to all nodes of triangular mesh in order defined by initial global nodes numeration, the following operation needs to be performed.

$$\bar{u} = \mathbf{RZ}\{\mathbf{P}\bar{u}_p\} \tag{15}$$
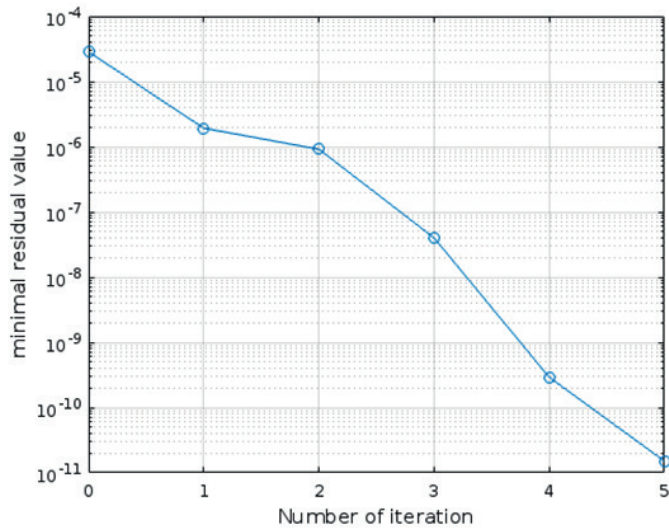
where $\mathbf{P}$ is a Cuthill-McKee permutation matrix.

www.czasopisma.pan.pl   PAN   www.journals.pan.pl

Computationally efficient method for determining the most important electrical parameters of Axial Field Permanent Magnet machine

Fig. 5. Minimum residual values obtained for solving a system after full preconditioning

Fig. 7. Magnetic field distribution in 2D, calculated using the presented method under no current conditions

The resulting distribution of vector potential $\vec{A}$, (having one component is a scalar field, hence it will be denoted as A_z in the following part) calculated under no current conditions, considering only the influence of permanent magnets for a cross section presented in Fig. 2, is presented in a Fig. 6.

All parameters, which are of interests here, can be calculated directly based on the distribution of potential A_z, determined for proper conditions. This is going to be discussed in the next section, however the distributions of $\vec{H}$ and $\vec{B}$ fields has also been calculated in accordance with equations 2–4, mainly for visualization purposes, and are presented in Fig. 7.

Obtained results are in line with the expectations. The closed loop path containing a magnetic flux is created by both solid iron rotor yokes and four permanent magnets mounted, as it was described in subsection 2.1
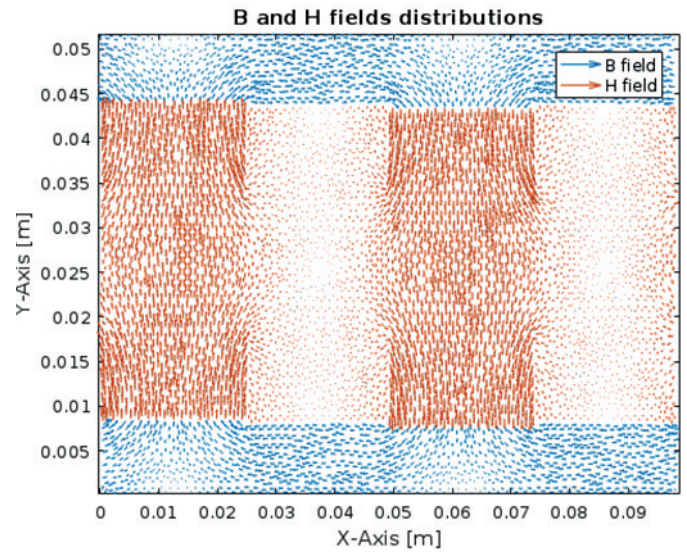
2.5. Determining the parameters of interest. If it comes to dynamic properties of AFPM machine, the most important electrical parameters are the values of stator phase winding self-inductance coefficients and magnetic flux coupled with a stator phase winding as a function of rotation angle. Determination of those values is the purpose of presented efforts.

2.5.1. Magnetic flux coupled with phase winding. To determine the values of magnetic flux coupled with a phase winding, only a single calculation of potential field A_z is needed. The coupled magnetic flux is later calculated as an algebraic sum of the potential A_z integrated over the areas of cross sections belonging to a single coil of corresponding phase with a sign corresponding to a direction of current flow. It presents as follows:

$$\Psi_A = \iint_{A^+} A_z\,dxdy - \iint_{A^-} A_z\,dxdy, \tag{16}$$

$$\Psi_B = \iint_{B^+} A_z\,dxdy - \iint_{B^-} A_z\,dxdy, \tag{17}$$

$$\Psi_C = \iint_{C^+} A_z\,dxdy - \iint_{C^-} A_z\,dxdy. \tag{18}$$

To compute these values as functions of rotation angle, the presented calculations have been repeated with an angular step equal to 0.8 of electrical degree. Obtained results are presented in Fig. 8.

The waveforms of an EMF, induced in generator phase windings, are directly proportional to the derivative of magnetic fluxes coupled with the phase windings after the rotation angle. Such derivatives have been calculated numerically using central finite difference approximation.

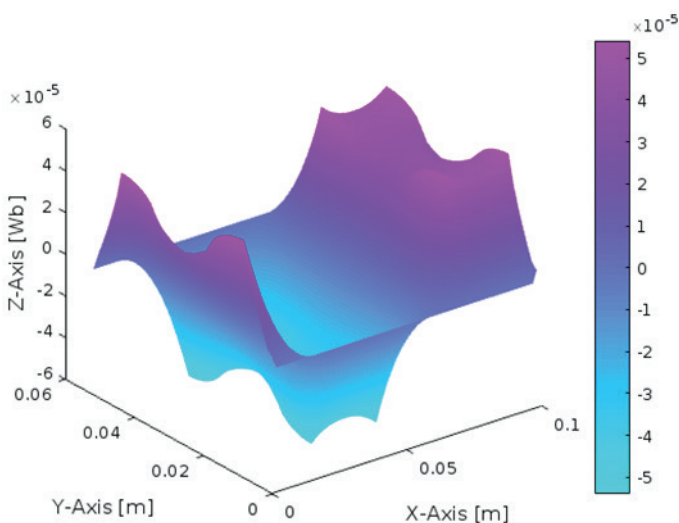$$f'(x) \approx \frac{f(x+h) - f(x-h)}{2h}. \tag{19}$$

Fig. 6. The distribution of a potential A calculated under non current conditions, considering only the influence of permanent magnets
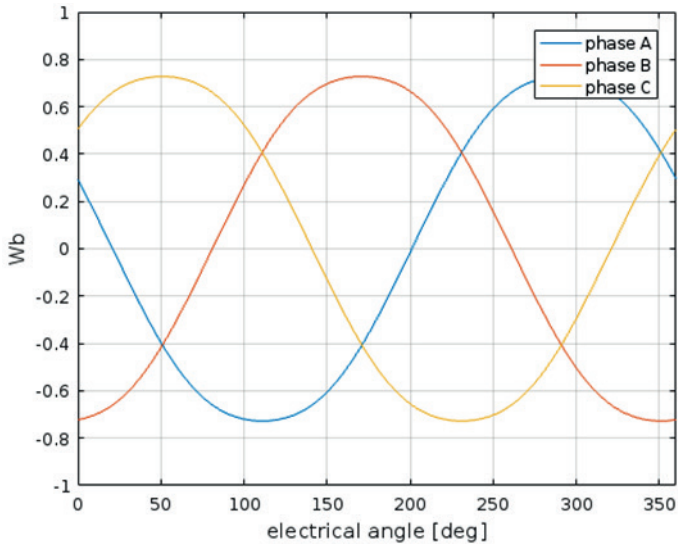
Fig. 8. The waveforms of magnetic fluxes coupled with the stator phase winding of AFPM machine

The results have been multiplied by the number of coils in phase connected in series, which is 16 in the presented case. Obtained waveforms are presented in Fig. 9.
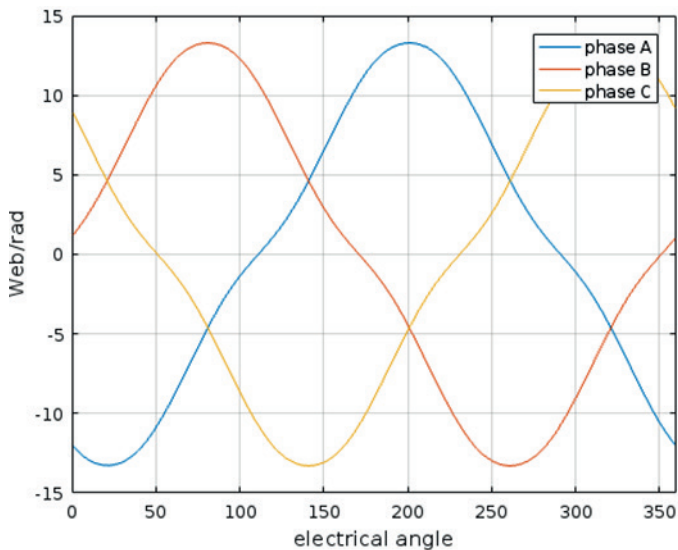

Fig. 9. The waveforms of the derivatives of magnetic fluxes coupled with the stator phase winding of AFPM machine, after the rotation angle

2.5.2. Calculations of the inductance coefficients.

In order to determine the values of self and mutual inductances of AFPM machine using presented method without assuming an ideal symmetry in advance, the distribution of vector potential field A_z needs to be calculated three times. For each calculation the current with density equal to $1^A/_{m^2}$ is assumed to be applied

as an excitation to one of the phases, while there is no current applied to the remaining two. Based on the resulting A_z, exemplary, if the excitation is applied to phase A, the corresponding inductance coefficients are computed as follows:

$$L_{aa} = \frac{W_n}{A_c} d \left[\iint_{A^+} A_z \, dx \, dy - \iint_{A^-} A_z \, dx \, dy \right], \quad (20)$$

$$L_{ab} = \frac{W_n}{A_c} d \left[\iint_{A^B} A_z \, dx \, dy - \iint_{B^-} A_z \, dx \, dy \right], \quad (21)$$

$$L_{ac} = \frac{W_n}{A_c} d \left[\iint_{C^+} A_z \, dx \, dy - \iint_{C^-} A_z \, dx \, dy \right], \quad (22)$$

where:
- W_n – number of wires in a single coil $[-]$,
- A_c – area of coil cross section $[m^2]$,
- d – coil active length $[m]$.

It needs to be pointed out that all values, which are interpreted as an energy when determined by $2D$ analysis, are related to the unity value in a z dimension. For this reason, in the equations above, the factor d represents the length of coils parts in a z dimension, which are represented in a $2D$ model as cross sections. The structure of the induction of matrix coefficients $\mathbf{L}$, as well as their values obtained using described method, are as follows:

$$\mathbf{L} = \begin{bmatrix} L_{aa} & L_{ab} & L_{ac} \\ L_{ba} & L_{bb} & L_{bc} \\ L_{ca} & L_{cb} & L_{cc} \end{bmatrix}. \quad (23)$$

The values of induction coefficients have been calculated using presented method, for both overlapping and non-overlapping stator winding. The results are presented below in a given order.

$$\mathbf{L} = \begin{bmatrix} 0.007062 & -0.0023723 & -0.0023723 \\ -0.0023723 & 0.007062 & -0.0023723 \\ -0.0023723 & -0.0023723 & 0.007062 \end{bmatrix} [H] \quad (24)$$

$$\mathbf{L} = \begin{bmatrix} 0.00987 & -7.84 \cdot 10^{-4} & -7.84 \cdot 10^{-4} \\ -7.84 \cdot 10^{-4} & 0.00987 & -7.84 \cdot 10^{-4} \\ -7.84 \cdot 10^{-4} & -7.84 \cdot 10^{-4} & 0.00987 \end{bmatrix} [H] \quad (25)$$

3. Validation of developed code

In order to check the correctness of the obtained results, the full 3D FEA has been conducted using Ansys/Maxwell software. The analysis was performed for both overlapping and non overlapping winding topologies. Experimental tests have been also conducted for further validation of all simulation re-

sults. As it was mentioned in section 2.1, the 3D FEA has the advantage to handle the whole magnetic field distribution inside the AFPM machine, including the overlapping end connection region. For that reason, the 3D FEA results are considered as the most accurate.

3.1. 3D Finite element model of AFPM machine. The 3D model of the machine without upper rotor yoke plate, is presented in Fig. 10. The permanent magnets, mounted within 3 mm thick aluminium ring, are visible on the top and the coils of overlapping three phase stator winding are located below. The disk shaped element located in the centre is made of solid iron and it constitutes a fixing of stator disk, which is made of epoxy resin and is not included in the model.

In Fig. 11, it is presented how the coils are interlaced in the front part, creating, at the same time, a thin system in an active part, over which permanent magnets are moved.
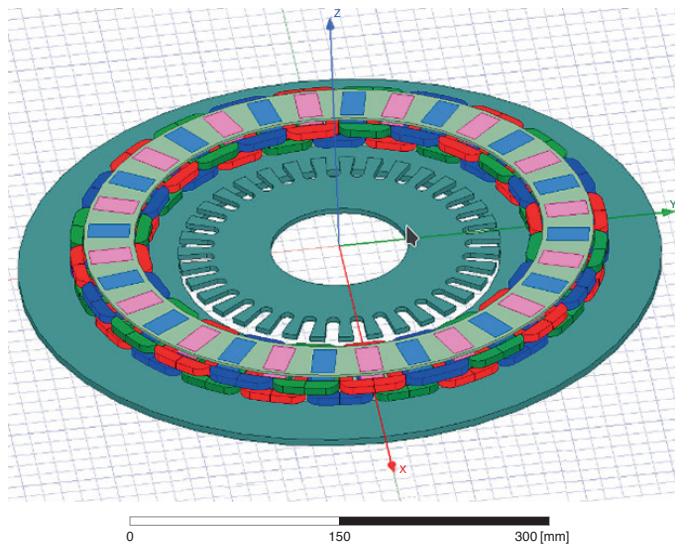

Fig. 10. The 3D model of analysed coreless axial field permanent magnet machine, presented without upper rotor yoke plate
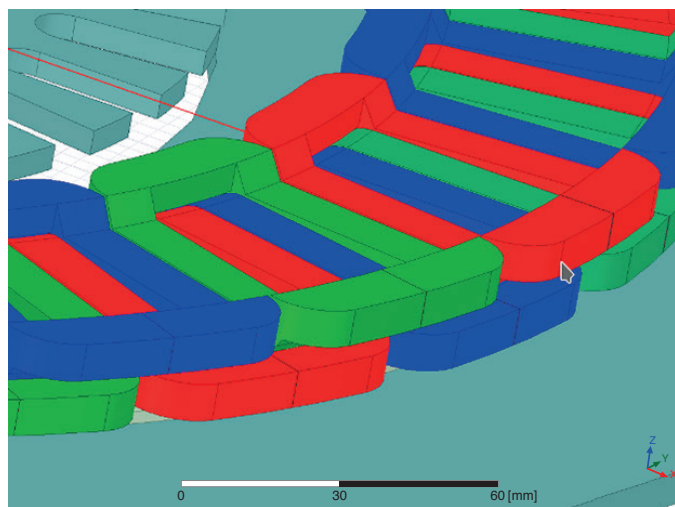

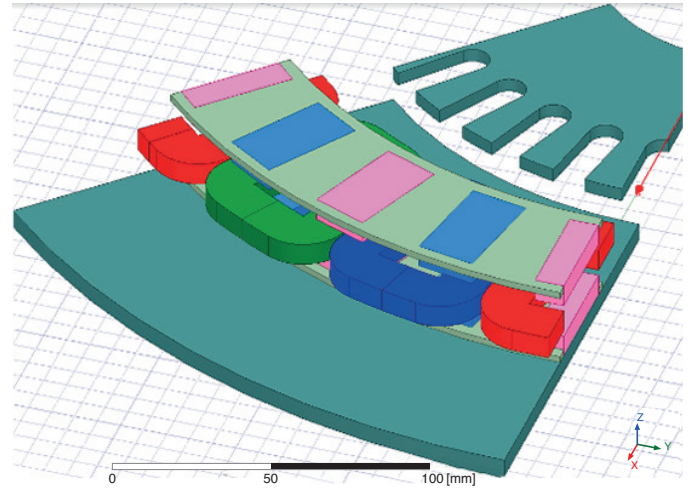Fig. 11. The view of three phase overlapping stator winding in a close up

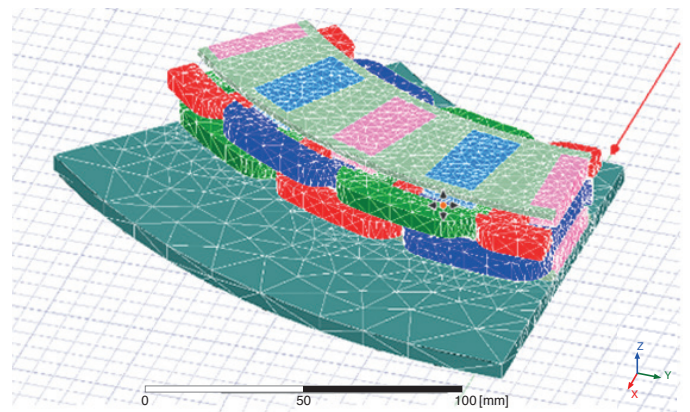Fig. 12. The view of a three phase non-overlapping stator winding, two poles section

Fig. 13. Triangular mesh providing, for a subjected model, an accuracy of determining the magnetic field energy at 0.1%

As it was mentioned in section 2.1, due to the overlapping construction of stator winding, the 1/8 of machine model needs to be analysed in a 3D approach. In case of non overlapping winding, the same pole pitch was analysed to preserve a cohesion of the comparison. The layout of coils are presented in Fig. 12. To respect the symmetry of the machine, a 'matching boundary' condition has been applied. After conducting simulation experiments, the discretization providing the magnetic field energy error at 0.1% has been chosen to apply. The triangular mesh obtained for a model section is presented in Fig. 13. The results obtained by performing the magneto static computations for presented 3D model using Ansys/Maxwell software will be compared with these obtained by the tested method in the next section.

3.2. Comparative study of obtained results.

3.2.1. Calculations of magnetic flux coupled with stator winding. In Fig. 14 the magnetic field distribution over the cylindrical cutting surface, placed in the middle of coil active
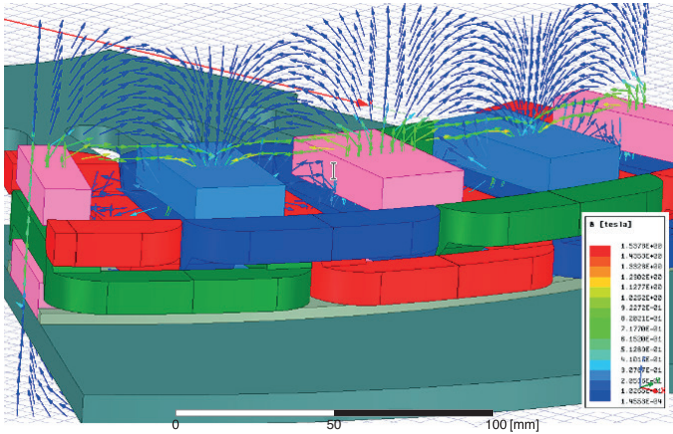
Fig. 14. The distribution of magnetic induction vector on a cylindrical cutting surface, placed in the middle of coil active part

part, is presented. The cross section presented in Fig. 2 section 2.1 corresponds to the half part of the same plane.

Comparing the obtained magnetic field distribution with the one presented in Fig. 7 section 2.4, it can be concluded that in both cases the boundary conditions, as well as the directions of magnetization vectors, have been applied correctly. In Fig. 15 the distribution of a magnetic field over a radially placed cutting plane is presented. The cross section contains a permanent magnet and an overlapping one as well as connection regions of the stator winding.
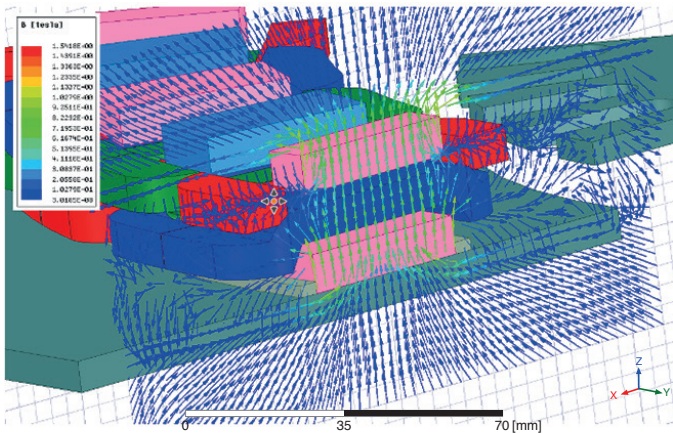

Fig. 15. The distribution of magnetic field over a radial cutting plane, placed in the middle of permanent magnet, presenting a significant magnetic coupling in the end connection regions of overlapping stator winding

It can be noticed that for an overlapping construction of stator winding, the magnetic coupling in the end connection region of coils is significant. This is considered as an impediment to use a 2D method for analysis of such constructions. Based on obtained field distributions, the magnetic flux coupled with stator phase winding and the values of self and mutual inductances have been calculated as a function of rotational angle

using Ansys/Maxwell software. In Fig. 16 the comparison of the results obtained using simplified 2D method and 3D analysis are presented.
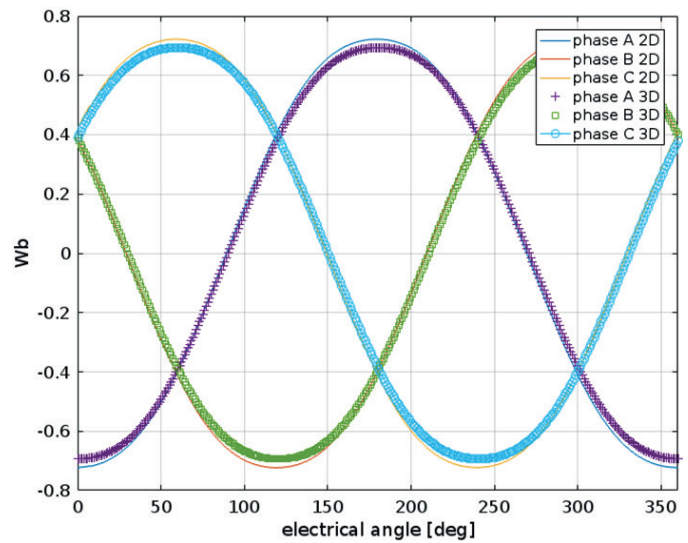

Fig. 16. The waveforms of magnetic flux coupled with phase winding, calculated using the presented simplified 2D method in comparison with the results of 3D FEA

The results prove that 2D method determines the overall shape of the subjected waveform. A slight inaccuracy concerns mainly the value of the amplitude, which is overestimated. In Fig. 17 the same plots are shown in a close-up.
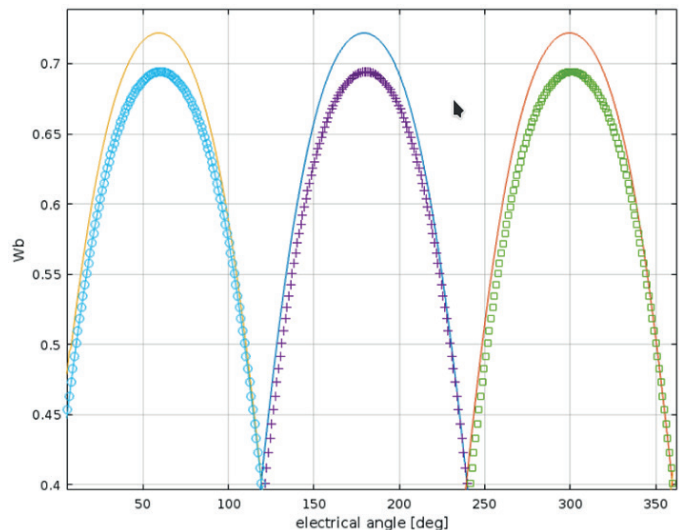

Fig. 17. The slight overestimation of the magnetic flux coupled amplitude occurring in comparison to the 3D FEA results

Because of its crucial meaning the same comparison has been performed for a derivatives of magnetic flux. The results are presented in Figs. 18 and 19.

www.czasopisma.pan.pl   PAN   www.journals.pan.pl

Computationally efficient method for determining the most important electrical parameters of Axial Field Permanent Magnet machine
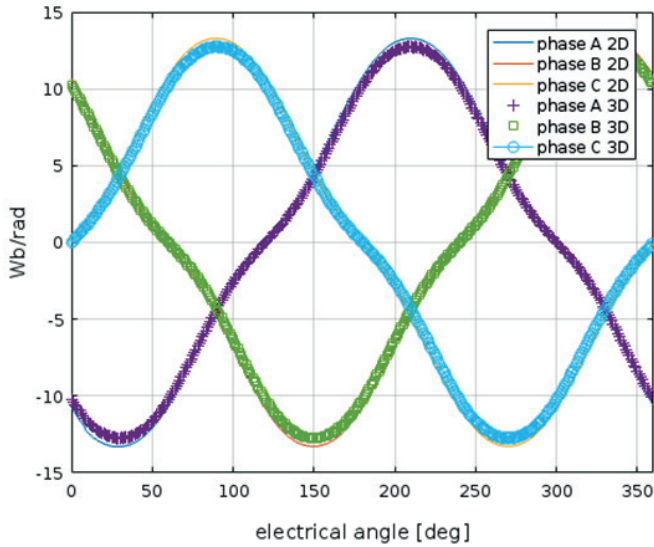
Fig. 18. The comparison of $\frac{\partial \Psi}{\partial \theta}$ waveforms obtained using simplified 2D and full 3D FEA
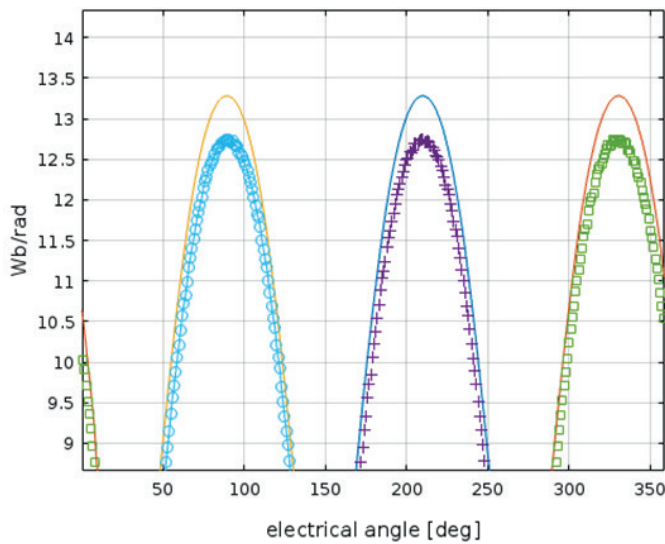

Fig. 19. The slight overestimation of the magnetic flux coupled amplitude occurring in comparison to the 3D FEA results

In accordance with the expectations, the derivatives of obtained waveform are in line with the 3D FEA results. For the proper accuracy assessment, the relative L^2 norm of error has been calculated for magnetic flux and its derivative as follows.

$$L_r^2 = \sqrt{\frac{\sum\limits_{k=0}^{n}\left(y_{3D_k} - y_{2D_k}\right)^2}{\sum\limits_{k=0}^{n} y_{3D_k}}} \qquad (26)$$

The results are presented in Table 4.

3.3.2. Calculations of self and mutual inductances coefficients. Both self and mutual inductance coefficients have been

calculated as a function of rotation angle using Ansys/Maxwell software. The results obtained for the overlapping winding are presented in the Figs. 20 and 21 respectively. The same results, but for non-overlapping type of stator winding, are presented in the Figs. 22 and 23. The slight periodic variability of the induction coefficients results are caused by the magnetic permeability of permanent magnets, which relative value is given in Table 1. The noticeable noise in the obtained waveforms is related to the numerical approximation errors. For a better readability the noise has been filtered out from the results presented in the corresponding figures.
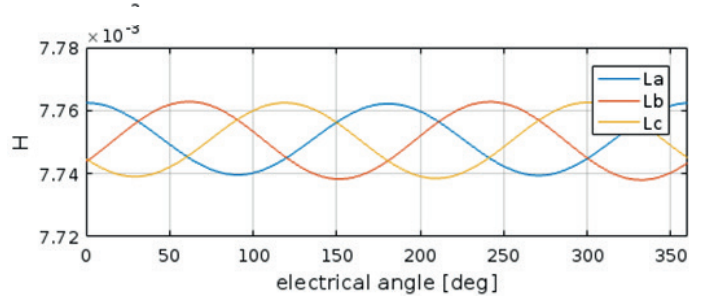

Fig. 20. The values of phase self inductance coefficients as a function of rotation angle, calculated for overlapping stator winding: original results (up) without the numerical approximation noise (down)
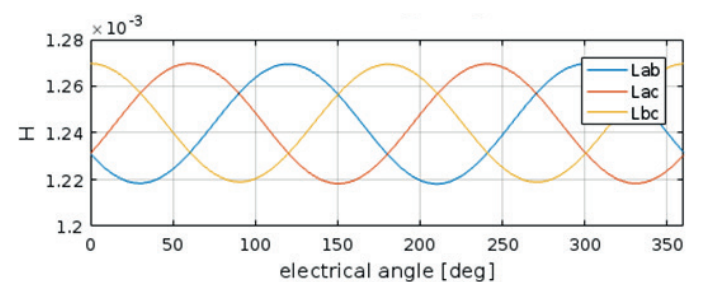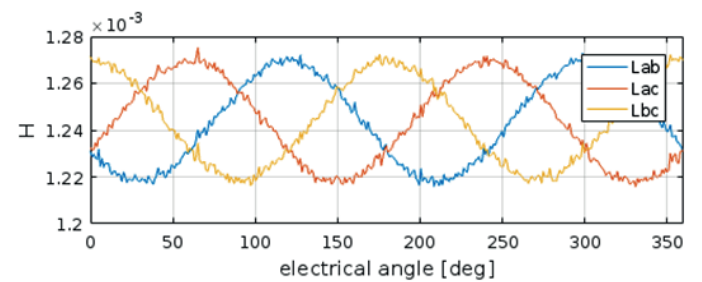
Fig. 21. The values of mutual inductance coefficients as a function of rotation angle, calculated for overlapping stator winding: original results (up) without the numerical approximation noise (down)
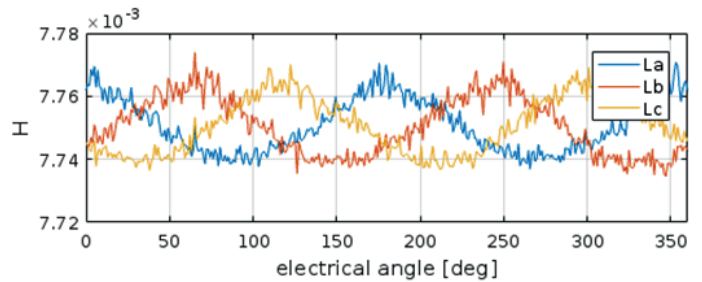
Fig. 22. The values of phase self inductance coefficients as a function of rotation angle, calculated for Non-overlapping stator winding: original results (up) without the numerical approximation noise (down)

Fig. 23. The values of mutual inductance coefficients as a function of rotation angle, calculated for Non-overlapping stator winding: original results (up) without the numerical approximation noise (down)
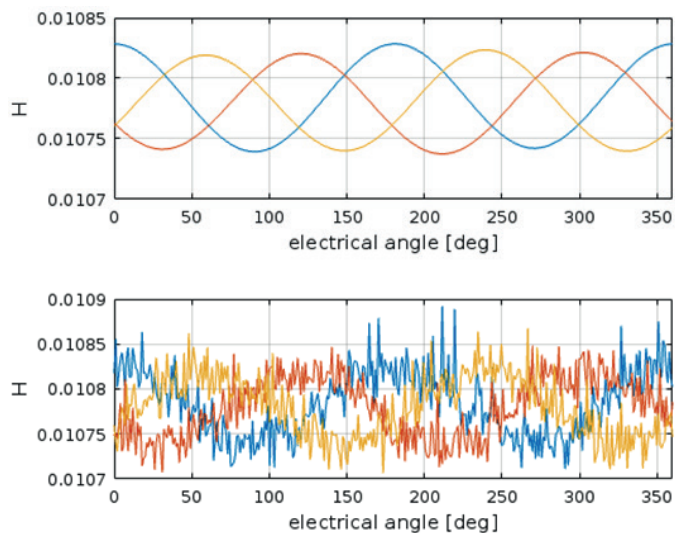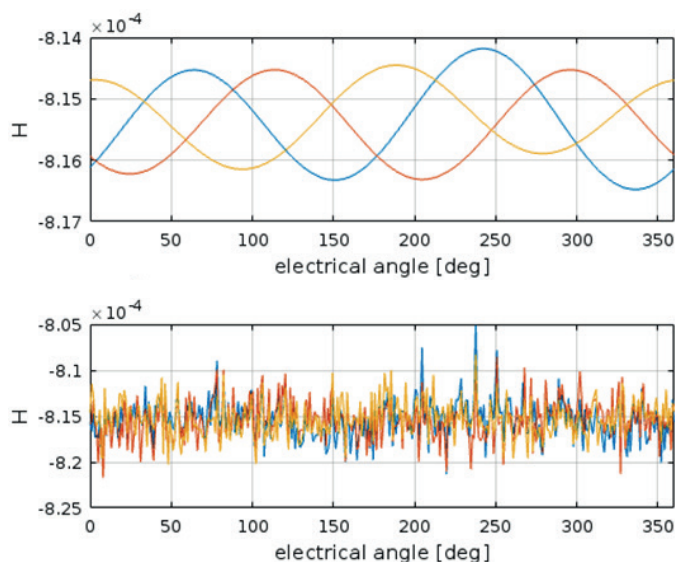
The amplitudes of the obtained waveforms are not bigger than $1 \cdot 10^{-5} H$ and $2 \cdot 10^{-5} H$. In any practical purposes such value is negligible hence the inductance coefficients of analysed AFPM machine, in case of self and mutual inductances respectively, can be considered as constant functions of rotation angle. The resulting value of phase self inductance coefficient can be adopted as $0.00775 H$ and $0.00124 H$ for the mutual one. It needs to be pointed, out that the value obtained for a phase self-inductance using the proposed method was noticeably lower. Moreover, in accordance with the expectations, due to the influence of the inductance of the end connections, which cannot be handled in the 2D approach, the values of mutual

inductance coefficients are divergent. To dispel the doubts, the experimental tests have been carried out on the prototype of the AFPM machine.

3.2.3. Results of experimental tests. In order to verify the above results, the measurements of generator inductance have been carried out using the GW Instek LCR-8110G measuring bridge, which allows impedance measurements over a wide frequency range. The measured values of the phase inductance as a function of frequency are presented in Fig. 24.
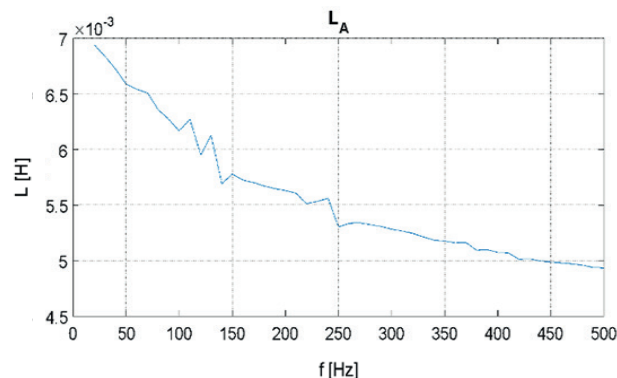

Fig. 24. The measured values of phase inductance of analysed AFPM machine, as a function of frequency

The results showed that the value of the phase inductance is strongly dependent on frequency. The eddy current losses take place in a solid iron rotor yokes as well as permanent magnets [17], which also strongly affect the results. Moreover, these phenomenona make the series connected to the R-L model of the circuit, which is implemented in GW Instek LCR-8110G measuring the bridge software and inconsistent with reality. For these reasons, further measurements have been conducted at frequency 20 Hz, at which the influence of Eddy current losses is slight. The measurements have been carried out for a single phase as well as for two phases connected by a neutral point. It needs to be pointed out that to refer the measured values to the results of magnetostatic calculations, it is needed to extrapolate it towards zero in a frequency domain. Using a simple linear extrapolation of values measured in a range of frequence between 20H to 50H, one can obtain 0.00776, which gives almost the exact convergence with the 3D FEA results. Based on the results, the value of mutual inductance has been calculated as follows:

$$L_m = \frac{1}{2}(L_A + L_B - L_s) \qquad (27)$$

where:
- L_A and L_B are the values of phase inductances,
- L_s is the value of inductance of two phases connected in series by the neutral point.

The values are presented in Table 2.

In order to experimentally verify the correctness of calculations of magnetic flux coupled with stator windings, the output

www.czasopisma.pan.pl　PAN　www.journals.pan.pl

Computationally efficient method for determining the most important electrical parameters of Axial Field Permanent Magnet machine

Table 2
Comparison of the results obtained for overlapping winding

parameter	value	unit
proposed algorithm		
phase self inductance	7.06	mH
mutual inductance	−2.372	mH
amplitude of magnetic flux coupled Ψ	0.72723	Wb
amplitude of $\frac{\partial \Psi}{\partial \theta}$	13.282	$\frac{Wb}{rad}$
THD of Ψ	3.6957	%
THD of $\frac{\partial \Psi}{\partial \theta}$	11.491	%
full 3D Finite Element Analysis		
phase self inductance	7.75	mH
mutual inductance	1.24	mH
amplitude of magnetic flux coupled Ψ	0.69408	Wb
amplitude of $\frac{\partial \Psi}{\partial \theta}$	12.747	$\frac{Wb}{rad}$
THD of Ψ	3.936231	%
THD of $\frac{\partial \Psi}{\partial \theta}$	11.888819	%
measurements		
phase self inductance	6.93863	mH
mutual inductance	1.073155	mH
Inductance of two series connected phases	11.7053	mH
extrapolated phase self inductance	7.76	mH

line voltage waveform in idle mode has been measured at constant speed 32.764 rotations per minute. The screenshot of the oscilloscope is presented in Fig. 25.
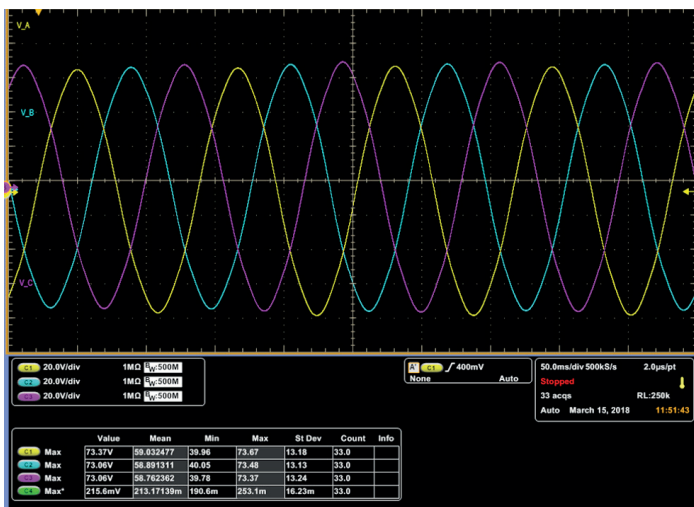

Fig. 25. Idle mode output line voltages measured at constant speed 32.764 rotations per minute

3.3. Summary comparison of computed and measured parameters of AFPM machine. The values of electrical parameters obtained for a machine with an overlapping type of winding, using: proposed algorithm, full 3D FEA as well as the results of measurements, are presented in Table 2. Additionally some selected results, in case of non overlapping stator winding, are presented in Table 3.

Table 3
Comparison of the results obtained for Non-overlapping winding

parameter	value	unit
tested method		
phase self inductance	0.00987	H
mutual inductance	$-7.84 \cdot 10^{-4}$	H
full 3D Finite Element Analysis		
phase self inductance	0.0108	H
mutual inductance	$8 \cdot 10^{-4}$	H

In order to provide an experimental verification of the calculated Ψ waveform, the simulation model of AFPM dynamic was developed using parameter values determined above. However, the description of the model is beyond of the scope of this paper it has been used to simulate the idle work mode of AFPM machine. The waveforms of the output line voltages, obtained at a constant rotation speed 32.764, have been compared with the measurements and are presented in Fig. 26.
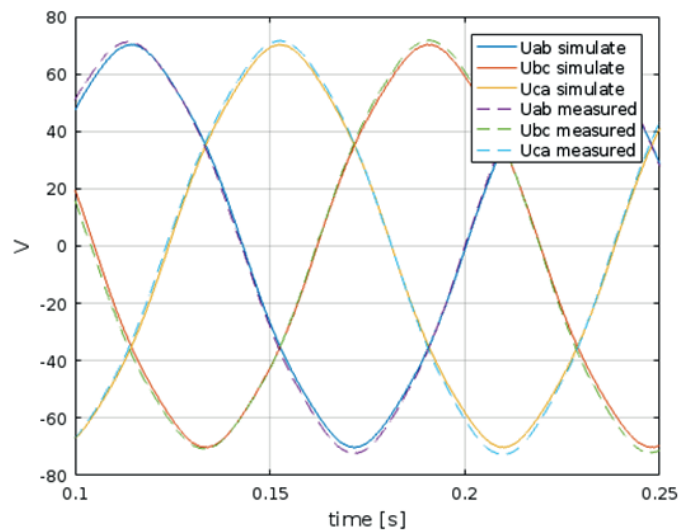

Fig. 26. Idle mode output line voltages measured at constant speed 32.764 rpm, in comparison with simulation results

The simulation results show a very good convergence with measurements, proving the correctness of computations when it comes to magnetic flux coupled with stator winding. The relative L_r^2 norm, calculated for a differences between 2D and 3D Ψ

and $\frac{\partial \Psi}{\partial \theta}$ waveforms in accordance with equation 26 is listed in Table 4. The relative differences between measured and calculated values of self and mutual inductances are presented in Table 5.

Table 4
Relative differences between values of magnetic flux coupled with stator windings calculated using 3D FEA and proposed algorithm

parameter	value	unit
Ψ		
relative L^2 norm	0.051925	[−]
Amplitude relative difference	0.047749	[−]
$\frac{\partial \Psi}{\partial \theta}$		
relative L^2 norm	0.0548	[−]
Amplitude relative difference	0.042028	[−]

Table 5
Relative differences between measured and computed values of inductances, given in % of measured value

parameter	value	unit
phase self inductance		
Overlapping winding – tested method	**−9.07**	%
Non-overlapping winding – tested method	**−8.62**	%
Overlapping winding 3D FEA	1.55	%
Non-overlapping winding 3D FEA	−1.22	%
mutual inductance		
Overlapping winding – tested method	**divergent**	[−]
Non-overlapping winding – tested method	**2.03**	%
Overlapping winding 3D FEA	2.12	%
Non-overlapping winding 3D FEA	1.93	%

The inaccuracy of the self-inductance value, obtained by 3D FEA, is mostly a result of differences between machine prototype and its 3D model. The values of induction coefficients, obtained by the usage of 2D method, are noticeably lower. It is caused by the omission of the impact of the end winding leakage inductance. This situation reveals the need to elaborate a computationally efficient method of determining the value of end winding leakage inductance, to improve the accuracy of developed program. In accordance with the expectations, proposed method is inherently unable to determine the values of mutual inductances when considered overlapping type of stator winding. This configuration of windings has been intentionally chosen for algorithm validation purposes because it is considered as the most inconvenient for application of the 2D approach. The quasi 3D approach [17] has also been tested, by taking a several cutting planes as slices. However, in considered case (rectangular shaped magnets and coils) the decreasing of

the error was almost negligible. If it comes to incorporation of the presented algorithm into a numerical optimization procedure, the consumption of computational time is crucial. It needs to be pointed out that to compute all the presented results less than 5 seconds is needed, while for the presented accuracy of calculations using 3D FEA for a single rotor position about 14 minutes are needed. That gives a total computational time about 9h 50 min. for the presented results.

4. Conclusions

The purpose of the efforts was to develop a computationally efficient code for determining the most important electrical parameters of AFPM machine. After several other experiments the simplified 2D FE algorithm with a single model set in cartesian coordinates was chosen to use. This approach has the advantage of being relatively easy to implement and use without any sophisticated software tools, although there are also other methods worth to be tested [18, 19]. Developed program has been validated by comparison with the results of full 3D FEA and the experiments conducted using a machine prototype, for both overlapping and non-overlaping topology of stator winding. The obtained results allow to state that due to its low time consumption, presented approach is well suited to incorporate in a numerical optimisation procedure of AFPM construction, especially if it comes to non overlapping winding topology, or if the optimisation criteria is subjected to back EMF. However, the inaccuracies in determining the values of induction coefficients make the method useful only for a rough calculations. The method stil can be used on a preliminary stage of a multidimensional numerical optimisation process to significantly shorten the overall time consumption The computational efficiency is particularly important when multi variable optimisation is conducted, using some modern algorithms such as: PSO [20], GA [21], or ABC. The development of fast method for numerical support of design processes has a great importance for designing the machines best suited for particular applications [22, 23].

References

[1] N. Radwan-Praglowska, D. Borkowski, and T. Węgiel, "Model of coreless axial flux permanent magnet generator", *Electrical Machines SME 18–21 June 2017,* IEEE Explore, 27 July, (2017).

[2] C. Gu, W. Wu, and K. Shao, "Magnetic field analysis and optimal design of DC permanent magnet coreless disc machine", *IEEE Trans. Magn*. 30 (5), 3668–3671, 1994.

[3] S. Piasecki, R. Szmurlo, J. Rabkowski, and M. Jasinski, "Dedicated system for design, analysis and optimization of AC-DC converters", *Bull. Pol. Ac.: Tech.* 64 (4), 2016.

[4] F. Caricchi, F. Crescimbini, A.D. Napoli, and E. Santini, "Optimal CAD-CAE design of axial flux permanent magnet motors", in *Proc. ICEM'92*, pp. 637–641. Paris, France, 1992.

[5] M. J. Kamper, R.-J. Wang, and F.G. Rossouw, "Analysis and performance of axial flux permanent magnet machine with air-cored non-overlapping concentrated stator windings", *IEEE Transactions on Industry Applications* 44 (5), (2008).

[6] M. Kamper, F.S. van der Merwe, and S. Wiliamson, "Direct finite element design optimisation of the cageless reluctance synchronous machine", *IEEE Transactions on Energy Conversion* 11 (3), September (1996).

[7] S. Berhausen and S. Paszek, "Use of the finite element method for parameter estimation of the circuit model of a high power synchronous generator", *Bull. Pol. Ac.: Tech.* 63 (3), 575–582, (2015).

[8] R.-J. Wang, M. J. Kamper, K. Van der Westhuizen, and J.F. Gieras "Optimal design of a coreless stator axial flux permanent magnet machine", *IEEE Transactions on Magnetics* 41 (1), (2005).

[9] A. Mlot, M. Lukaniszyn, and M. Korkosz "Influence of an end-winding size on proximity losses in a high-speed PM synchronous motor", *Selected Problems of Electrical Engineering and Electronics,* 2015.

[10] D. Vanoost, H. De Gersem, J. Peuteman, G. Gielen, and D. Pissort, "Two dimensional magnetic finite- element simulation for devices with a radial symmetry", *IEEE Transactions On Magnetics* 50 (5), 2014.

[11] D. Engwirda, *MESH2D: Delaunay-based mesh generation in MATLAB,* 2017.

[12] P.P. Silvester and R.L. Ferrari, *Finite Elements for Electrical Engineers*, 3rd Edition, 1996.

[13] J.M. Jin, *The Finite Element Method in Electromagnetics*, Wiley – IEEE 3rd Edition, 2014.

[14] J. Li and Y.-T. Chen, *Computational Partial Differential Equations Using Matlab*, Springer, September (2010).

[15] M.N.O. Sadiku, *Numerical Techniques in Electromagnetics with MATLAB*, 3rd Edition, 2009.

[16] Y. Saad, "GMRES: A generalized minimal residual algorithm for solving non symmetric linear systems", *SIAM J. Sci. Stat. Comput.* 7, 856–869, (1986).

[17] R.-J. Wang and M.J. Kamper, "Calculation of Eddy Current Loss in Axial Field Permanent-Magnet Machine With Coreless Stator", *IEEE Transactions on Energy Conversion* 19 (3), (2004).

[18] Y.-P. Yang, Ch.-H. Lee, and P.-Ch. Hung, "Multiobjective optimal design of an axial-flux permanent-magnet wheel motor for electric scooters",vol. 8 (1), 1–12, 2014.

[19] J.R. Bumby, R. Martin, M.A. Mueller, E. Spooner, N.L. Brown, and B.J. Chalmers, "Electromagnetic design of axial-flux permanent magnet machines", *IEEE Electric Power Applications* 151 (2), 2004.

[20] G. Cvetkovski and L. Petkovska, "Efficiency Improvement of Axial Flux PM Motor Using Particle Swarm Optimisation", *Przegląd Elektrotechniczny*, ISSN 0033–2097, r. 89 nr 2b/2013.

[21] G. Cvetkovski, L. Petkovska, and S. Gair, "Genetic Algorithm Applied in Optimal Design of PM Disc Motor Using Specific Power as Objective", *Computational Methods for Electrical Devices Design*, SCI 327, pp. 229–246, Springer-Verlag Berlin Heidelberg 2010.

[22] M. Gwozdzik, M. Krystkowiak, C. Jedrzejczak, A. Gulczynski, and D. Matecki, "Generator with modulated magnetic flux for wind turbines", *Bull. Pol. Ac.: Tech.* 65 (4), 469–478, (2017).

[23] A. Moradewicz and M. Kazmierkowski, "High efficiency contactless energy transfer system with power electronic resonant converter", *Bull. Pol. Ac.: Tech.* 57 (4), 2010.